

Lawrence Berkeley National Laboratory

LBL Publications

Title

Surfactants are Ineffective for Reducing Imbibition of Water-Based Fracturing Fluids in Deep Gas Reservoirs

Permalink

<https://escholarship.org/uc/item/7nq9r2hw>

Journal

Energy & Fuels, 35(14)

ISSN

0887-0624

Authors

Tokunaga, Tetsu K
Omosebi, Omotayo A
Wan, Jiamin

Publication Date

2021-07-15

DOI

10.1021/acs.energyfuels.1c01162

Peer reviewed

1 **Surfactants are ineffective for reducing imbibition of water-based fracturing fluids in deep**
2 **gas reservoirs**

3

4 Tetsu K. Tokunaga*, Omotayo A. Omosebi, and Jiamin Wan

5 Energy Geosciences Division, Lawrence Berkeley National Laboratory

6 Berkeley, California, USA

7

8 **ABSTRACT:** Minimizing loss of injected hydraulic fracturing fluids into shale along fracture-
9 matrix boundaries is desired because imbibed water restricts gas production and wastes valuable
10 water resources. This problem has motivated the addition of surfactants into water-based
11 hydraulic fracturing fluids in order to reduce the capillary driving force for imbibition. Here, we
12 show that reduction in interfacial tension and wettability alteration have negligible ability to
13 reduce imbibition in deep gas reservoirs. The effectiveness of altering capillary forces acting at
14 the wetting front also depends on the injection pressure acting at the fracture-matrix boundary.
15 The pressure at the interface between the fracture and the shale matrix is constrained between the
16 reservoir pore pressure and formation pressure (rock fracture pressure, also known as breakdown
17 pressure of the rock) and increases with depth to magnitudes that greatly exceed that of capillary
18 pressures. The analyses presented here show that even maximum alteration of interfacial
19 properties that result in strongly hydrophobic interactions between the fracturing fluid and
20 reservoir rock is incapable of significantly reducing imbibition in deep reservoirs. Instead of
21 using surfactants, this analysis points to decreases in wellbore shut-in pressures and shut-in times
22 as practical options for reducing imbibition losses of water-based fluids.

23 *Corresponding author: Tetsu K. Tokunaga, tktokunaga@lbl.gov

24 1. INTRODUCTION

25 Hydraulic fracturing for stimulating production of low-permeability shale gas reservoirs uses
26 large volumes of water, often exceeding 10^4 m³ per well, while competing for valuable water
27 resources and incurring high costs for water supply and treatment of flowback water¹⁻³. In
28 addition to these burdens, loss of water-based fracturing fluids into reservoir matrix rocks during
29 shut-in impedes production through blocking pores and through structural damage within the
30 wetted fracture-matrix interface zone^{1, 4-6}. The adverse effects of water imbibition into shales
31 have motivated investigations on ways to minimize water loss within reservoirs through
32 manipulating interfacial properties and capillary forces. Indeed, a key strategy advanced in
33 stimulating unconventional gas reservoirs is to use surfactants in hydraulic fracturing fluids in
34 order to reduce the capillary pressure driving imbibition and thereby decrease thicknesses of
35 water-blocked zones at the fracture-matrix interface⁷⁻¹⁶. Indeed, in enhanced oil recovery (EOR),
36 the applications of surfactants to reduce surface tension, stabilize microemulsions, and alter
37 reservoir wettability to facilitate oil mobilization are well recognized¹⁷⁻²². It is worth noting that
38 surfactants are also added into hydraulic fracturing fluids for controlling rheological properties.
39 As essential components of foams and gelling agents, surfactants can help enhance viscosity,
40 thereby increase fracture width and improve proppant delivery²³⁻²⁵.

41 Instead of revisiting the extensively studied and complex problem of surfactant
42 applications in EOR, the analyses developed here reexamines the importance of changing
43 capillary forces in the context of hydraulic fracturing in deep gas reservoirs. To the best of our
44 knowledge, a critical limitation of all the previous studies on surfactant applications for
45 controlling imbibition in shale gas reservoirs is that influences of high reservoir pressures and
46 temperatures were not considered. For a typical depth of 2.5 km for a horizontal well²⁶, hydraulic

47 fracturing occurs at pressures and temperatures of about 35 MPa and 80 °C, and in the following
48 we show that such conditions severely limit the extent to which changing capillary forces can
49 influence frac fluid imbibition in gas reservoirs.

50 Before considering capillary effects, it is worth briefly noting that electric double layer
51 expansion and osmotic potential gradients can also influence imbibition in clay-rich, saline
52 sediments. Although correlations between clay content, salinity, and imbibition rates have been
53 obtained²⁷⁻²⁹, and osmotic potentials associated with saline reservoir pore waters have been
54 determined³⁰, challenges persist for quantifying their actual impacts under reservoir conditions. A
55 limitation associated with interpreting how clay swelling impacts imbibition is that experiments
56 to date have largely been conducted on unloaded or only uniaxially loaded cores. Lack of total
57 confinement allows multidimensional sample expansion during hydration, producing highly
58 transmissive microfracture networks that artificially enhance imbibition relative to that actually
59 occurring under in-situ reservoir stresses. Indeed, such free swelling leads to artificial
60 microfracturing and even break up of unconfined samples^{10, 28, 31}. The importance of applying
61 confining stresses during imbibition tests on shales is underscored by closure of microfractures
62 during hydration experiments conducted under isotropic confinement³².

63 The extent to which imbibition can be facilitated by osmotic forces also requires better
64 understanding because shales are not ideal semi-permeable membranes. The osmotic pressure
65 gradient driving imbibition is moderated by the osmotic efficiency, σ , which ranges from 0 to 1,
66 and depends inversely on the product of characteristic pore-size times the square-root of salt
67 concentration³³. The inverse dependence on the square-root of salinity diminishes σ to less than
68 0.01 as salinities increase above 1 mol L⁻¹ in monovalent waters³³⁻³⁷, and small fractions of
69 divalent cations lower σ even further³⁸. Thus, measurements of σ for shale systems are needed in

70 order to evaluate the significance of osmotically driven imbibition³⁹, and confinement of shale
71 samples during such measurements is again warranted for preventing microfracturing.

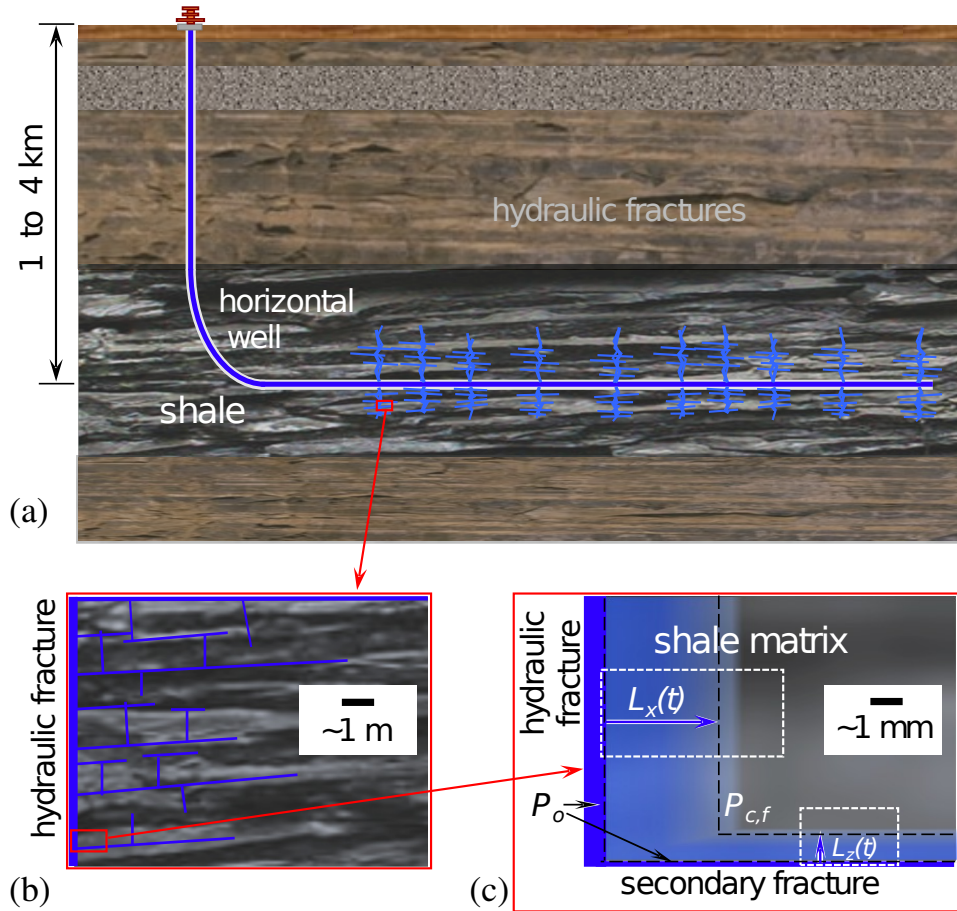
72 The analyses developed here compare two basic driving forces for imbibition, capillary
73 forces acting at the imbibition front and the hydrostatic reservoir pressure acting at the fracture-
74 matrix boundary. Through comparing both of these forces, the effectiveness of manipulating
75 interfacial properties will be shown to have a strong dependence on both depth and permeability,
76 such that surfactant use in deep reservoirs has negligible ability to reduce imbibition.

77

78 2. METHODOLOGY

79 Because a one-dimensional analysis of transient imbibition will be used to compare influences of
80 matrix rock capillarity and pressures in fractures, we first provide justification for this
81 simplification of the geometry of fluids entering reservoirs through complex networks of
82 hydraulic fractures and natural fractures. A conceptual model of how fracturing fluids are
83 distributed shortly after hydraulic fracturing is shown in Figure 1, with (a) the km scale overview
84 of multiple hydraulic fractures within a single fracturing stage, (b) a m scale depiction of a
85 region including both a hydraulic fracture and numerous secondary fractures (natural and
86 stimulated) supplied with frac fluid via main hydraulic fractures, and (c) a mm scale close-up
87 view of water imbibing into shale matrix from a vertical hydraulic fracture and secondary
88 (natural or stimulated) horizontal fracture. In the days following fracturing and prior to gas
89 production from reservoirs with matrix permeability k in the range of 10^{-21} to 10^{-17} m² (n-Darcy to
90 10 μ -Darcy), imbibition fronts only propagate beyond the fracture-matrix interface to distances
91 in the range of mm to cm into the matrix⁴⁰. When such short penetration distances are small
92 relative to characteristic distances between the fractures, water imbibition occurs locally as an

93 effectively one-dimensional process emanating from complex fracture networks. Therefore, in
 94 the analysis developed next, flow is represented as being effectively one-dimensional.



95
 96 **Figure 1.** Conceptual model of hydraulic fracturing fluid injection into shale gas reservoir. (a)
 97 Cross-section along horizontal well showing water distribution via nominally vertically oriented
 98 hydraulic fractures. (b) Local region adjacent to a hydraulic fracture, showing water injected into
 99 network of horizontal and vertical fractures (both natural and stimulated). (c) Injected water
 100 imbibing into a portion of shale matrix bounded by a vertical hydraulic fracture and a secondary
 101 horizontal fracture, both with fluid pressure P_o . This close-up shows the orientation-dependent
 102 imbibition front distances $L_i(t)$ at which the capillary pressure is $P_{c,f}$.

103

104 At the local scale of shale matrix adjacent to a fracture (microfracture) supplied with
 105 hydraulic fracturing fluid, the pressure difference acting across the advancing wet matrix of
 106 thickness $L(t)$ is the sum of the pressure at the fracture-matrix interface P_o and the capillary
 107 pressure at the advancing wetting front, $P_{c,f}$. Because of strongly anisotropic k in shales⁴¹, $L(t)$
 108 generally exhibits orientation-dependence as indicated in Figure 1c. We will show later that
 109 anisotropy can be included through use of k components perpendicular and parallel to bedding
 110 planes, but does not impact conclusions concerning alteration of $P_{c,f}$. Thus for simplicity, we
 111 consider isotropic k , and a pressure gradient acting across the expanding imbibition zone given
 112 by $(P_{c,f} + P_o)/L$. The transient Darcy equation for 1-dimensional flow in the step-function wetting
 113 zone approximation is

$$114 \quad J = \frac{\Delta \theta dL}{dt} = \frac{k}{\mu} \frac{P_o + P_{c,f}}{L} \quad (1)$$

115 where J is the volumetric flow of water per unit area, $\Delta \theta$ is the volumetric water content increase
 116 within the wetted zone, t is time, and μ is the viscosity of the fracturing fluid. Rearrangement and
 117 integration of eq 1 gives the time-dependent thickness of the wet zone
 118

$$119 \quad L(t) = \sqrt{\frac{2k}{\mu \Delta \theta} (P_o + P_{c,f}) \sqrt{t}} \quad (2)$$

120
 121 Because the cumulative volumetric water flux per unit area $I(t) = \Delta \theta L(t)$, the local volumetric
 122 imbibition rate per unit area of fracture-matrix contact area is expressed in the Green-Ampt
 123 model^{40, 42, 43} as

$$124 \quad I(t) = \sqrt{\frac{2 \Delta \theta k}{\mu} (P_{c,f} + P_o) \sqrt{t}} \quad (3)$$

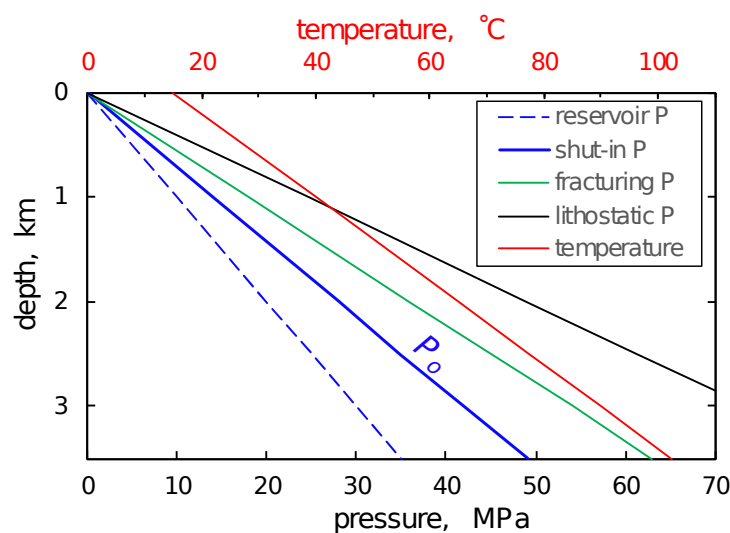
125 The Green-Ampt equation results directly from Darcy's law applied to the migration of an
 126 imbibition front characterized by constant $P_{c,f}$, and precedes the practically identical Lucas-

127 Washburn equation describing flow in capillaries^{44, 45}, and an equivalent later model by Handy⁴⁶
128 that is commonly used in petroleum recovery research^{10, 47-50}. The Green-Ampt model also
129 predates other studies on soils that have highlighted the square-root of time dependence of
130 imbibition, where the first grouped square-root term on the right-hand side of eq 3 is the
131 sorptivity S ⁵¹, a parameter now also coming into use for characterizing imbibition in
132 hydrocarbon reservoir rocks⁵²⁻⁵⁴. In both the Green-Ampt and Handy models, the relative
133 permeability function is not needed because early stages of imbibition under positive pressure
134 (and especially at high pressure) at the Darcy continuum scale proceeds at rates close to that
135 resulting from single phase flow. Recently, it was shown that imbibition measurements used to
136 determine S also provide reasonable estimates of k over a range of measured k that spanned 10
137 orders of magnitude⁴⁰. The fact that the database used to develop the S - k correlation included
138 shales suggests that osmotic effects did not significantly enhance imbibition rates into those very
139 low k samples.

140 Given that k and $\Delta\theta$ of a given reservoir are relatively fixed, the controllable variables
141 available for reducing imbibition are μ , $P_{c,f}$, P_o , and t . While eq 3 clearly shows that thickeners
142 used to increase μ for proppant transport cause decreases in fluid imbibition, rheological
143 properties of fracturing fluids are largely designed with fracture generation and proppant
144 transport in mind⁵⁵. Therefore, our focus here will be on examining the significance of potential
145 changes to $P_{c,f}$, particularly in comparison to P_o . From eq 3, $P_{c,f}$ and P_o act additively within the
146 square-root term to drive imbibition. Thus, the magnitude of $P_{c,f}$ relative to P_o determines the
147 relative importance of surfactant additions on reducing imbibition. It is worth noting that the
148 equivalent effects that $P_{c,f}$ and P_o have in driving imbibition are evident from their additive
149 influences in eq 3, and have been supported by experimental tests conducted over ranges of

150 elevated injection pressures^{56, 57}. For the purpose of this study, we focus on the relative
 151 magnitudes of $P_{c,f}$ and P_o under commonly employed laboratory spontaneous imbibition
 152 experiments and under field reservoir conditions.

153 Newly generated fractures experience elevated fracturing pressures that are depth-
 154 dependent. Following shut-in, P_o begins to decline back towards the reservoir pressure⁵⁸. Thus,
 155 values of P_o are depth-dependent, being greater than the reservoir pressure and less than the rock
 156 fracture pressure. For purposes of this study, the hydrostatic gradient for reservoir pressure was
 157 taken as 10 MPa km⁻¹, the fracture gradient was taken as 18 MPa km⁻¹⁵⁹, and the wellbore shut-in
 158 P_o was assigned values midway between these limiting pressures. Thus, a hypothetical shut-in
 159 gradient of 14 MPa km⁻¹ was assumed, with P_o declining towards the reservoir pressure in the
 160 limit of very long shut-in times (Figure 2). It is important to note that reservoir pressures are very
 161 high in deep reservoirs, hence P_o remains high prior to the production phase. Also included in
 162 Figure 2 are a lithostatic pressure gradient of 24.5 MPa km⁻¹ and geothermal gradient of 25 °C
 163 km⁻¹.



164

165 **Figure 2.** Depth profiles of reservoir pressure, bottom hole shut-in pressure P_o , formation
166 fracture pressure, lithostatic pressure, and temperature. Surface pressures and temperature are 0
167 MPa and 15 °C, respectively.

168

169 The dependence of $P_{c,f}$ on k and depth was determined in three steps, for water-wet rock
170 with negligible variation in contact angle. The impact of wettability will be examined later in this
171 analysis. First, a correlation between k and the capillary pressure for air entry into hydrophilic
172 water-saturated porous materials $P_{c,a}$ was determined using data from the literature on room
173 temperature water-air systems (where interfacial tension $\gamma \approx 72$ mN/m)⁴⁰. The power-law
174 correlation given by

$$175 \quad P_{c,a}(0.1 \text{ MPa}, 20 \text{ }^\circ\text{C}) = (0.106 \text{ Pa m}^{0.72})k^{-0.36} \quad (4)$$

176 fits data on consolidated and unconsolidated media with a root mean-square deviation in $\log P_{c,a}$
177 of 0.71, for measurements spanning twelve orders of magnitude in k . In previous work, the same
178 data set was scaled with interfacial tension to estimate the methane gas-entry capillary pressure
179 $P_{c,g}$ for a reservoir at 70 °C and 20 MPa⁴⁰. Equation 4 was next multiplied by the previously
180 determined linear correlation⁴⁰ $P_{c,f} = 1.21P_{c,a}$ to obtain the dependence of $P_{c,f}$ on k at the ground
181 surface

$$182 \quad P_{c,f}(z=0, 0.1 \text{ MPa}, 20 \text{ }^\circ\text{C}) = \alpha k^{-0.36} \quad (5)$$

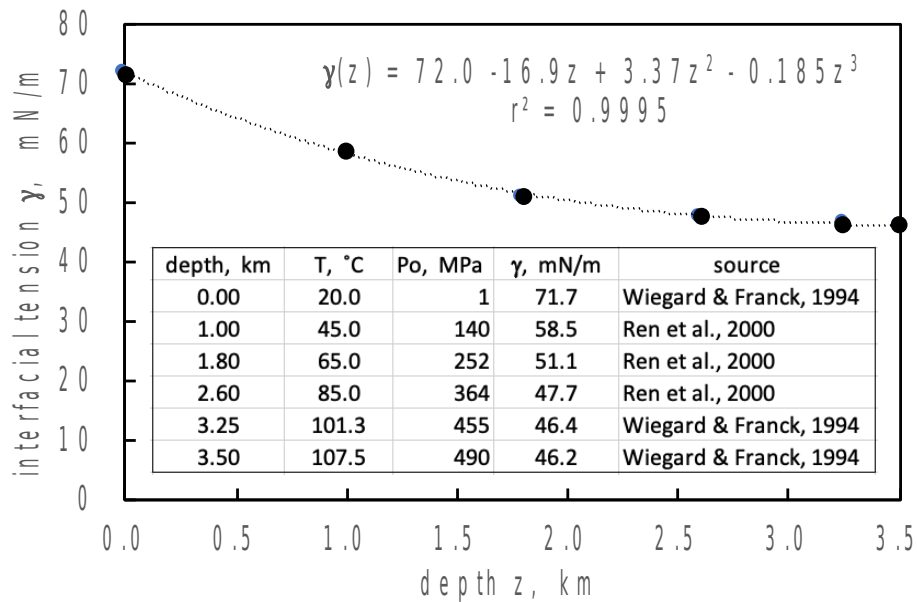
183 where $\alpha = 1.21 \times 0.106 \text{ Pa m}^{0.72} = 0.128 \text{ Pa m}^{0.72}$.

184 The final step needed to predict how $P_{c,f}$ varies with both depth and k requires
185 determining how the methane-water interfacial tension γ varies with depth z below the ground
186 surface. This relation was obtained by interpolating values of methane-water γ from the

187 literature^{60, 61} over a range of pressure-temperature combinations that are compatible with the P_o
 188 and T depth profiles illustrated in Figure 2.

189

190



191

192 **Figure 3.** Depth-dependence of methane-water γ , given the estimated temperature and wellbore
 193 shut-in pressure profiles.

194

195 These depth-dependent methane-water $\gamma(z)$ values were fit to $\gamma(z) = 72.0 - 16.9z + 3.37z^2 -$
 196 $0.185z^3$ shown in Figure 3, then used to scale Equation 5 in order to estimate how P_{cf} depends on
 197 both k and z

$$198 \quad P_{cf}(z,k) = [\gamma(z)/\gamma(0)]\alpha k^{-0.36} \quad (6)$$

199 where $\gamma(0) = 71.7 \text{ mN m}^{-1}$, the methane-water γ at the ground surface. Substituting the depth-
 200 dependent wellbore shut-in $P_o(z)$ and eq 6 into eq 3 gives:

201
$$I(t) = \sqrt{\frac{2 \Delta \theta k}{\mu} \left(\frac{\gamma(z)}{\gamma(0)} \alpha k^{-0.36} + Bz \right)} \sqrt{t} \quad (7a)$$

202 where $B = 14.0 \text{ MPa km}^{-1}$, the wellbore shut-in gradient. The impact of surfactants on $I(t)$ can
 203 then be expressed as

204
$$I(t) = \sqrt{\frac{2 \Delta \theta k}{\mu} \left(\frac{f\gamma(z)}{\gamma(0)} \alpha k^{-0.36} + Bz \right)} \sqrt{t} \quad (7b)$$

205 where f represents the fractional reduction in $\gamma(z)$ imparted by addition of surfactants. For
 206 example, reducing γ from 50 mN m^{-1} to 15 mN m^{-1} corresponds to $f = 0.3$. Thus, the impact of
 207 surfactant addition in reducing fracturing fluid imbibition relative to the unaltered fluid (with $f =$
 208 1) is given by

209
$$1 - \frac{I(f, z)}{I_0(z)} = 1 - \left[\frac{\frac{f\gamma(z)}{\gamma(0)} \alpha k^{-0.36} + Bz}{\frac{\gamma(z)}{\gamma(0)} \alpha k^{-0.36} + Bz} \right]^{0.5} \quad (8)$$

210 which we term the capillary alteration effectiveness (CAE). The CAE can range from 0 where
 211 the imbibed fluid volume is unaffected by the addition of surfactant, up to 1 where surfactant
 212 addition prevents any fluid imbibition into the reservoir due to extremely strong hydrophobic
 213 interaction. Note that anisotropy can be accommodated for imbibition perpendicular to and
 214 parallel to shale bedding planes by using suitable directional components of k in eq 8. Here, it is
 215 also convenient to consider how changing wettability can be incorporated into eq 8. Recall that
 216 P_c in a straight capillary tube of radius R is given by the Young–Laplace equation

217
$$P_c = \frac{2 \gamma \cos \theta}{R} \quad (9)$$

218 where θ is the contact angle. Although scaling of P_c by $\cos \theta$, in porous media is not generally
 219 accurate⁶², it serves as a useful approximation⁶³. By scaling P_c by both γ and $\cos \theta$, f can be

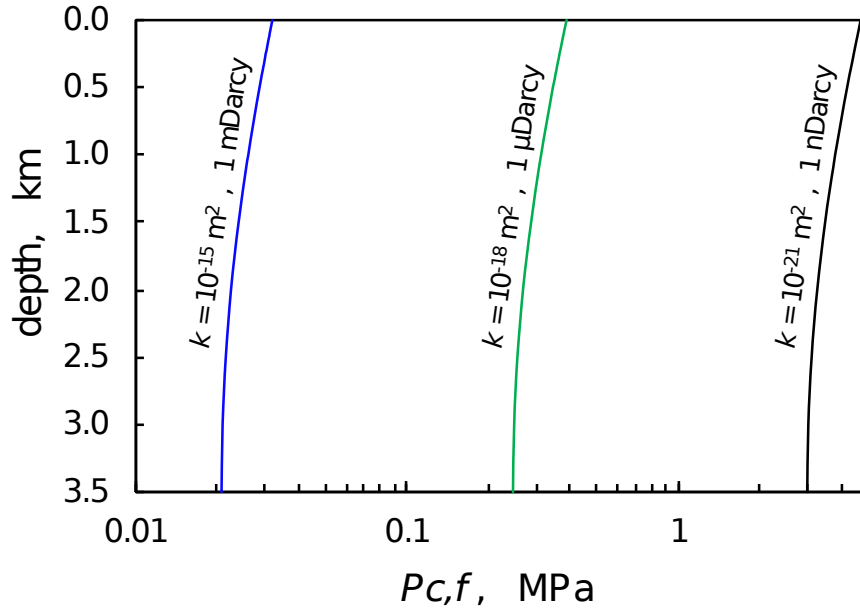
220 interpreted more generally to be the product of $\cos\theta$ times the relative reduction in γ . Such a
221 generalization allows examining the implications of a hypothetical extremely hydrophobic
222 interaction between the reservoir and fracturing fluid. Such a case, with $\theta = \pi$ and $\cos\theta = -1$ can
223 then be examined with $f = -1$, and captures the theoretical maximum impact achievable for
224 capillary alteration of imbibition. The full range of wetting behavior, including that of complex
225 mixed-wet systems^{64,65}, is encompassed by varying f from 1 (strongly hydrophilic) to -1 (strongly
226 hydrophobic). In order to focus on the potential impacts that weakening the capillary driving
227 force can have on imbibition, values of f that range from 0.3 to -1 will later be examined.

228

229 3. RESULTS AND DISCUSSION

230 The capillary pressure acting at the imbibition front, P_{cf} , depends on k , and decreases with depth
231 as approximated by eq 4. The strong k -dependence of P_{cf} shown in Figure 4 reflects the power-
232 law correlation with $k^{-0.36}$ (eq 5), which differs from $k^{-0.5}$ predicted from Leverett scaling^{40, 66}.
233 Decreases in γ with depth (Figure 3) account for the depth-dependence of P_{cf} .

234



235

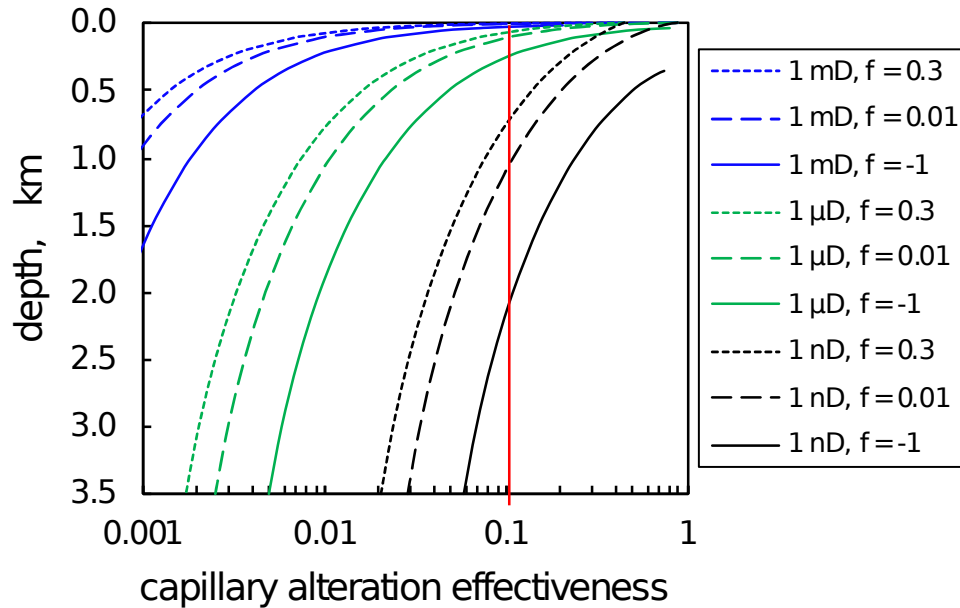
236 **Figure 4.** Depth-dependence of imbibition front $P_{c,f}$ for different k , showing that $P_{c,f}$ decreases
 237 with depth and is larger for lower k .

238

239 The CAE is both k - and depth-dependent, as illustrated in Figure 5, where depth profiles
 240 are plotted for $k = 10^{-15}$ (1 mDarcy), 10^{-18} (1 μ Darcy), and 10^{-21} m² (1 nDarcy), with interfacial
 241 tensions reduced by $f = 0.3$, 0.01, and -1. These three f values represent modest, very strong, and
 242 maximum possible decreases in the capillary driving force for imbibition, respectively.
 243 Influences of surfactant alteration can be more important in lower k reservoirs, e.g. shales,
 244 because their higher $P_{c,f}$ can be more effectively reduced with surfactant addition. However,
 245 capillary alteration effectiveness decreases with depth because the pressure at the fracture-matrix
 246 boundary P_o becomes large enough to be the dominant driving force, even in very low k
 247 reservoirs. The depths by which capillary alteration effectiveness diminishes to only 10% are
 248 reached where the profiles cross the vertical red line in Figure 5. Thus, even with interfacial
 249 tension reduced by $f = 0.01$, capillary alteration effectiveness is diminished by only 10% at

250 depths of 0.11 and 1.1 km, for 1 μ Darcy and 1 nDarcy reservoirs, respectively. At the much
 251 greater depths commonly stimulated with hydraulic fracturing, the effectiveness in reducing fluid
 252 imbibition with surfactants will be negligible. Figure 5 also shows that even if a 1 nDarcy
 253 reservoir was stimulated with a fluid that imparted extremely hydrophobic interactions ($\theta = \pi, f =$
 254 -1), the effectiveness in reducing imbibition would be limited to less than 10% at depths greater
 255 than 2.2 km. Because k is commonly larger parallel to shale bedding planes, Figure 5 shows that
 256 the CAE for imbibition from vertical fractures is far less than that for imbibition from horizontal
 257 fractures. Given that μ is generally optimized for proppant delivery, only decreases in P_o and t
 258 remain as controllable variables that have the capacity to significantly reduce imbibition during
 259 reservoir stimulation.

260



261

262 **Figure 5.** The effectiveness of altering interfacial forces in order to minimize fracturing fluid
 263 imbibition depends on reservoir k (1 mDarcy, 1 μ Darcy, 1 nDarcy) and depth. The parameter f in
 264 the legend represents the fractional reduction in water-gas surface tension achieved by addition

265 of surfactant. The cases with $f = -1$ represent the maximum reduction in capillary uptake
266 achievable with extremely hydrophobic interactions.

267

268 The shallow limit of $z = 0$ km in Figure 5 represents typical laboratory imbibition tests,
269 where water or fracturing fluids are commonly introduced with negligible pressure head, i.e. P_o
270 ≈ 0 MPa. Under negligible P_o , alteration of $P_{c,f}$ with surfactants results in clear decreases to
271 imbibition rates shown in recent studies⁹⁻¹². It is noteworthy that the contrasting effects of high
272 P_o (24 MPa) versus negligible P_o was recognized in comparisons of imbibition without and with
273 surfactants in a previous laboratory study on imbibition of fracturing fluids⁶⁷. Our analyses
274 generalizes such findings by showing how the depth-dependent P_o and k -dependent $P_{c,f}$ limit the
275 effectiveness that alterations of interfacial tension and wettability can have on imbibition.

276 CONCLUSION

277 Thicknesses of water-blocked regions along fracture-matrix interfaces grow by interfacial
278 tension-dependent capillarity acting at the advancing wetting front $P_{c,f}$, and by the fracturing fluid
279 pressure acting at the fracture-matrix boundary, P_o . Therefore, it is important to understand the
280 relative magnitudes of these driving forces in order to determine the effectiveness of surfactant
281 additions aimed at reducing the capillary contributions to imbibition. Our analyses show the
282 following.

- 283 • The extent to which surfactants can reduce imbibition is limited by the k -dependent
284 magnitude of $P_{c,f}$, and has greater potential effect in lower k reservoirs.
- 285 • Magnitudes of P_o in deep reservoirs are in the range of tens of MPa, and are greater than
286 $P_{c,f}$ values of even the lowest k reservoirs.

- 287 • Therefore, alteration of water-gas interfacial tension and wettability have negligible
288 ability to reduce imbibition of water-based fracturing fluids in deep, unconventional
289 reservoirs.
- 290 • Given that rheological properties of fracturing fluids are largely prescribed for the
291 purpose of delivering proppants into fractures, the remaining operational options for
292 minimizing imbibition and water block thicknesses are reducing shut-in times and
293 reducing the magnitude of P_o .

294

295

296 AUTHOR INFORMATION

297 Corresponding Author

298 Tetsu K. Tokunaga – Energy Geosciences Division, Lawrence Berkeley National Laboratory,

299 Berkeley, California 94720, United States

300 Email: tktokunaga@lbl.gov

301 Authors

302 Omotayo A. Omosibi – Energy Geosciences Division, Lawrence Berkeley National Laboratory,

303 Berkeley, California 94720, United States

304 Jiamin Wan – Energy Geosciences Division, Lawrence Berkeley National Laboratory, Berkeley,

305 California 94720, United States

306

307 ACKNOWLEDGMENTS

308 This work was supported by the Assistant Secretary for Fossil Energy, Office of Oil and Natural

309 Gas, through the National Energy Technology Laboratory under the U.S. Department of Energy

310 Contract No. DE-AC02-05CH11231. We thank the two reviewers for their helpful comments on

311 the manuscript, John Selker (Oregon State University) for comments on a recent publication⁴⁰

312 that helped motivate this study, and Stephen Henry (NETL) for project management.

313

314 REFERENCES

- 315 1. Edwards, R. W. J.; Doster, F.; Celia, M. A.; Bandilla, K. W., Numerical modeling of gas
 316 and water flow in shale gas formations with a focus on the fate of hydraulic fracturing fluid.
 317 *Environmental Science & Technology* **2017**, *51* (23), 13779-13787.
- 318 2. Vengosh, A.; Jackson, R. B.; Warner, N.; Darrah, T. H.; Kondash, A., A critical review
 319 of the risks to water resources from unconventional shale gas development and hydraulic
 320 fracturing in the United States. *Environmental Science & Technology* **2014**, *48* (15), 8334-8348.
- 321 3. Rosa, L.; Rulli, M. C.; Davis, K. F.; D'Odorico, P., The water-energy nexus of hydraulic
 322 fracturing: A global hydrologic analysis for shale oil and gas extraction. *Earths Future* **2018**, *6*
 323 (5), 745-756.
- 324 4. Chenevert, M. E.; Osisanya, S. O., Shale swelling at elevated temperature and pressure.
 325 In *Rock Mechanics, Proc. 33rd U.S. Symposium*, Tillerson, J. R.; Wawersik, W. R., Eds.
 326 Balkema: Rotterdam, 1992; pp 869-878.
- 327 5. Holditch, S. A., Factors affecting water blocking and gas-flow from hydraulically
 328 fractured gas wells. *Journal of Petroleum Technology* **1979**, *31* (12), 1515-1524.
- 329 6. Bennion, D. B.; Thomas, F. B., Formation damage issues impacting the productivity of
 330 low permeability, low initial water saturation gas producing formations. *J Energ Resour-Asme*
 331 **2005**, *127* (3), 240-247.
- 332 7. Chai, Y.; Li, X.; Jing, D., Application of surfactants in hydraulic fracturing for enhanced
 333 oil/gas recovery. *Oil & Gas Research* **2019**, *5* (1), 1-10.
- 334 8. Hussien, O. S.; Elraies, K. A.; Almansour, A.; Husin, H.; Belhaj, A.; Ern, L.,
 335 Experimental study on the use of surfactant as a fracking fluid additive for improving shale gas
 336 productivity. *Journal of Petroleum Science and Engineering* **2019**, *183*.
- 337 9. Roychoudhuri, B.; Tsotsis, T. T.; Jessen, K., An experimental investigation of
 338 spontaneous imbibition in gas shales. *Journal of Petroleum Science and Engineering* **2013**, *111*,
 339 87-97.
- 340 10. Makhanov, K.; Habibi, A.; Dehghanpour, H.; Kuru, E., Liquid uptake of gas shales: A
 341 workflow to estimate water loss during shut-in periods after fracturing operations. *Journal of*
 342 *Unconventional Oil and Gas Resources* **2014**, *7*, 22-32.
- 343 11. Das, S.; Adeoye, J.; Dhiman, I.; Bilheux, H. Z.; Ellis, B. R., Imbibition of mixed-charge
 344 surfactant fluids in shale fractures. *Energy & Fuels* **2019**, *33* (4), 2839-2847.
- 345 12. Sun, Y. P.; Bai, B. J.; Wei, M. Z., Microfracture and surfactant impact on linear
 346 cocurrent brine imbibition in gas-saturated shale. *Energy & Fuels* **2015**, *29* (3), 1438-1446.
- 347 13. Gdanski, R., Modeling the impact of capillary pressure reduction by surfactants. In *SPE*
 348 *International Symposium on Oilfield Chemistry*, Society of Petroleum Engineers: Houston, TX,
 349 2007; p 7.
- 350 14. Chee, S. C.; Hidayat, B. M.; Mohshim, D. F.; Zain, Z. M.; Chai, I. C. H.; Borhan, N.;
 351 Ismail, H. H.; Adam, M., Evaluation of anionic and non-ionic surfactant performance for
 352 Montney shale gas hydraulic fracturing fluids. *Journal of Petroleum Exploration and Production*
 353 **2021**, *11* (4).
- 354 15. Penny, G. S.; Pursley, J. T., Field study of completion fluids to enhance gas production in
 355 the Barnett Shale. In *SPE Gas Technology Symposium*, Society of Petroleum Engineers: Calgary,
 356 Alberta, Canada, 2006; p 10.

- 357 16. Liang, T. B.; Xu, K.; Lu, J.; Nguyen, Q.; DiCarlo, D., Evaluating the performance of
358 surfactants in enhancing flowback and permeability after hydraulic fracturing through a
359 microfluidic model. *SPE Journal* **2020**, *25* (1), 268-287.
- 360 17. Hirasaki, G. J.; Miller, C. A.; Puerto, M., Recent advances in surfactant EOR. *SPE*
361 *Journal* **2011**, *December 2011*, 889-907.
- 362 18. Sheng, J. J., Status of surfactant EOR technology. *Petroleum* **2015**, *1*, 97-105.
- 363 19. Alzobaidi, S.; Da, C.; Tran, V.; Prodanovic, M.; Johnston, K. P., High temperature
364 ultralow water content carbon dioxide-in-water foam stabilized with viscoelastic zwitterionic
365 surfactants. *J. Colloid Interface Sci.* **2017**, *488*, 79-91.
- 366 20. Sheng, J. J., What type of surfactants should be used to enhance spontaneous imbibition
367 in shale and tight reservoirs? *Journal of Petroleum Science and Engineering* **2017**, *159*, 635-643.
- 368 21. Levitt, D. B.; Jackson, A. C.; Heinson, C.; Britton, L. N.; Malik, T.; Dwarakanath, V.;
369 Pope, G. A., Identification and evaluation of high-performance EOR surfactants. *Spe Reserv Eval*
370 *Eng* **2009**, *12* (2), 243-253.
- 371 22. Burrows, L. C.; Haeri, F.; Cvetic, P.; Sanguinito, S.; Shi, F.; Tapriyal, D.; Goodman,
372 A.; Enick, R. M., A Literature review of CO₂, natural gas, and water-based fluids for enhanced
373 oil recovery in unconventional reservoirs. *Energy & Fuels* **2020**, *34* (5), 5331-5380.
- 374 23. Elsner, M.; Hoelzer, K., Quantitative Survey and Structural Classification of Hydraulic
375 Fracturing Chemicals Reported in Unconventional Gas Production. *Environmental Science &*
376 *Technology* **2016**, *50* (7), 3290-3314.
- 377 24. Montgomery, C., Fracturing fluid components. In *Effective and Sustainable Hydraulic*
378 *Fracturing*, Bungler, A. P.; McLennan, J.; Jeffrey, R., Eds. InTech: Rijeka, Croatia, 2013; pp 25-
379 45.
- 380 25. Al-Muntasheri, G. A., A critical review of hydraulic-fracturing fluids for moderate- to
381 ultralow-permeability formations over the last decade. *Spe Prod Oper* **2014**, *29* (4), 243-260.
- 382 26. Jackson, R. B.; Lowry, E. R.; Pickle, A.; Kang, M.; DiGiulio, D.; Zhao, K. G., The
383 depths of hydraulic fracturing and accompanying water use across the United States.
384 *Environmental Science & Technology* **2015**, *49* (15), 8969-8976.
- 385 27. Yang, L.; Dou, N. H.; Lu, X. B.; Zhang, X. H.; Chen, X.; Gao, J.; Yang, C. W.;
386 Wang, Y., Advances in understanding imbibition characteristics of shale using an NMR
387 technique: a comparative study of marine and continental shale. *J Geophys Eng* **2018**, *15* (4),
388 1363-1375.
- 389 28. Ge, H. K.; Yang, L.; Shen, Y. H.; Ren, K.; Meng, F. B.; Ji, W. M.; Wu, S.,
390 Experimental investigation of shale imbibition capacity and the factors influencing loss of
391 hydraulic fracturing fluids. *Petrol Sci* **2015**, *12* (4), 636-650.
- 392 29. Binazadeh, M.; Xu, M. X.; Zolfaghari, A.; Dehghanpour, H., Effect of electrostatic
393 interactions on water uptake of gas shales: The interplay of solution ionic strength and
394 electrostatic double layer. *Energy & Fuels* **2016**, *30* (2), 992-1001.
- 395 30. Zhou, Z.; Li, X. P.; Teklu, T. W., A critical review of osmosis-associated imbibition in
396 unconventional formations. *Energies* **2021**, *14* (4), 835.
- 397 31. Dehghanpour, H.; Lan, Q.; Saeed, Y.; Fei, H.; Qi, Z., Spontaneous imbibition of brine
398 and oil in gas shales: Effect of water adsorption and resulting microfractures. *Energy & Fuels*
399 **2013**, *27* (6), 3039-3049.

- 400 32. Zhang, S. F.; Sheng, J. J.; Shen, Z. Q., Effect of hydration on fractures and permeabilities
401 in Mancos, Eagleford, Barnett and Marcellus shale cores under compressive stress conditions.
402 *Journal of Petroleum Science and Engineering* **2017**, *156*, 917-926.
- 403 33. Bresler, E., Anion exclusion and coupling effects in nonsteady transport through
404 unsaturated soils .1. Theory. *Soil Science Society of America Journal* **1973**, *37* (5), 663-669.
- 405 34. Cey, B. D.; Barbour, S. L.; Hendry, M. J., Osmotic flow through a Cretaceous clay in
406 southern Saskatchewan, Canada. *Canadian Geotechnical Journal* **2001**, *38* (5), 1025-1033.
- 407 35. Neuzil, C. E.; Person, M., Reexamining ultrafiltration and solute transport in
408 groundwater. *Water Resour. Res.* **2017**, *53* (6), 4922-4941.
- 409 36. Barbour, S. L.; Fredlund, D. G., Mechanisms of osmotic flow and volume change in clay
410 soils. *Canadian Geotechnical Journal* **1989**, *26* (4), 551-562.
- 411 37. Al-Bazali, T. M.; Zhang, J.; Chenevert, M. E.; Sharma, M. M., Factors controlling the
412 membrane efficiency of shales when interacting with water-based and oil-based muds. In *SPE*
413 *International Oil & Gas Conference and Exhibition in China*, Society of Petroleum Engineers:
414 Beijing, China, 2006; p 11.
- 415 38. Tremosa, J.; Goncalves, J.; Matray, J. M., Natural conditions for more limited osmotic
416 abnormal fluid pressures in sedimentary basins. *Water Resour. Res.* **2012**, *48*, W04530.
- 417 39. Fakcharoenphol, P.; Torcuk, M.; Kazemi, H.; Wu, Y. S., Effect of shut-in time on gas
418 flow rate in hydraulic fractured shale reservoirs. *J Nat Gas Sci Eng* **2016**, *32*, 109-121.
- 419 40. Tokunaga, T. K., Simplified Green-Ampt model, imbibition-based estimates of
420 permeability, and implications for leak-off in hydraulic fracturing. *Water Resour. Res.* **2020**, *56*
421 (4), 12.
- 422 41. Gensterblum, Y.; Ghanizadeh, A.; Cuss, R. J.; Amann-Hildenbrand, A.; Krooss, B. M.;
423 Clarkson, C. R.; Harrington, J. F.; Zoback, M. D., Gas transport and storage capacity in shale
424 gas reservoirs – A review. Part A: Transport processes. *Journal of Unconventional Oil and Gas*
425 *Resources* **2015**, *12*, 87-122.
- 426 42. Green, W. H.; Ampt, G. A., Studies on soil physics Part I - The flow of air and water
427 through soils. *J Agr Sci* **1911**, *4*, 1-24.
- 428 43. Neuman, S. P., Wetting front pressure head in infiltration-model of Green and Ampt.
429 *Water Resour. Res.* **1976**, *12* (3), 564-566.
- 430 44. Lucas, R., The time law of the capillary rise of liquids. *Kolloid Z* **1918**, *23* (1), 15-22.
- 431 45. Washburn, E. W., The dynamics of capillary flow. *Physical Review* **1921**, *17* (3), 273-
432 283.
- 433 46. Handy, L. L., Determination of effective capillary pressures for porous media from
434 imbibition data. *Transactions of the American Institute of Mining and Metallurgical Engineers*
435 **1960**, *219* (5), 75-80.
- 436 47. Babadagli, T., Scaling capillary imbibition during static thermal and dynamic fracture
437 flow conditions. *Journal of Petroleum Science and Engineering* **2002**, *33* (4), 223-239.
- 438 48. Mason, G.; Morrow, N. R., Developments in spontaneous imbibition and possibilities for
439 future work. *Journal of Petroleum Science and Engineering* **2013**, *110*, 268-293.
- 440 49. Mehana, M.; Al Salman, M.; Fahes, M., Impact of salinity and mineralogy on slick water
441 spontaneous imbibition and fFormation strength in shale. *Energy & Fuels* **2018**, *32* (5), 5725-
442 5735.

- 443 50. Yang, R.; He, S.; Hu, Q. H.; Zhai, G. Y.; Yi, J. Z.; Zhang, L., Comparative
444 investigations on wettability of typical marine, continental, and transitional shales in the Middle
445 Yangtze Platform (China). *Energy & Fuels* **2018**, 32 (12), 12187-12197.
- 446 51. Philip, J. R., The theory of infiltration, 4. Sorptivity and algebraic infiltration equations.
447 *Soil Science* **1957**, 84, 257-264.
- 448 52. Yang, R.; Guo, X. S.; Yi, J. Z.; Fang, Z. X.; Hu, Q. H.; He, S., Spontaneous imbibition
449 of three leading shale formations in the Middle Yangtze Platform, South China. *Energy & Fuels*
450 **2017**, 31 (7), 6903-6916.
- 451 53. Yang, J.; Leng, J. Y.; Qiao, L. K.; Wang, L. L.; Ding, J. D., Parameter prediction of
452 water imbibition in unsaturated shales using the NMR method. *Geofluids* **2019**, 2019, 4254159.
- 453 54. Hatiboglu, C. U.; Karaaslan, U.; Akin, S., Spontaneous imbibition in low permeability
454 carbonates. *Energ Source* **2005**, 27 (9), 839-846.
- 455 55. Montgomery, C., Fracturing Fluids. In *Effective and Sustainable Hydraulic Fracturing*,
456 Bunger, A.; McLennan, J.; Jeffrey, R., Eds. Intech: Brisbane, Australia, 2013; p 23.
- 457 56. Yeh, W. W. G.; Franzini, J. B., Moisture movement in a horizontal soil column under
458 influence of an applied pressure. *Journal of Geophysical Research* **1968**, 73 (16), 5151-5157.
- 459 57. Pagels, M.; Willberg, D. M.; Edelman, E.; Zagorski, W.; Frantz, J., Quantifying
460 fracturing fluid damage on reservoir rock to optimize production. In *Unconventional Resources*
461 *Technology Conference*, URTEC: Denver, Colorado, 2013; p 9.
- 462 58. Nolte, K. G., Principles of fracture design based on pressure analysis. *SPE Production*
463 *Engineering* **1988**, (February), 22-30.
- 464 59. Bell, J. S.; Grasby, S. E., The stress regime of the Western Canadian Sedimentary Basin.
465 *Geofluids* **2012**, 12 (2), 150-165.
- 466 60. Wiegand, G.; Franck, E. U., Interfacial tension between water and non-polar fluids up to
467 473 K and 2800 bar. *Berichte der Bunsengesellschaft fur physikalische Chemie* **1994**, 98 (6),
468 809-817.
- 469 61. Ren, Q. Y.; Chen, G. J.; Yan, W.; Guo, T. M., Interfacial tension of (CO₂ + CH₄) +
470 water from 298 K to 373 K and pressures up to 30 MPa. *J. Chem. Eng. Data* **2000**, 45 (4), 610-
471 612.
- 472 62. Philip, J. R., Limitations on scaling by contact angle. *Soil Science Society America*
473 *Proceedings* **1971**, 35, 507-509.
- 474 63. Parlange, J.-Y., Scaling by contact angle. *Soil Science Society America Proceedings*
475 **1974**, 38, 161-162.
- 476 64. Salathiel, R. A., Oil recovery by surface film drainage in mixed-wettability rocks.
477 *Journal of Petroleum Technology* **1973**, 25 (Oct), 1216-1224.
- 478 65. Morrow, N. R.; Mason, G., Recovery of oil by spontaneous imbibition. *Curr. Opin.*
479 *Colloid Interface Sci.* **2001**, 6, 321-337.
- 480 66. Leverett, M. C., Capillary behavior in porous solids. *Transactions of the American*
481 *Institute of Mining and Metallurgical Engineers* **1941**, 142, 152-169.
- 482 67. Roychaudhuri, B.; Xu, J.; Tsotsis, T. T.; Jessen, K., Forced and spontaneous imbibition
483 experiments for quantifying surfactant efficiency in tight shales. In *SPE Western North American*
484 *and Rocky Mountain Joint Regional Meeting*, Society of Petroleum Engineers: Denver,
485 Colorado, USA, 2014; p 7.
- 486

487 **TOC Graphic**

488

489